

## Molecular-dynamics study of elasticity and failure of ideal solids

Zhen-Gang Wang

*Department of Chemistry, University of California at Los Angeles, 405 Hilgard Avenue,  
Los Angeles, California 90024*

Uzi Landman

*School of Physics, Georgia Institute of Technology, Atlanta, Georgia 30332*

Robin L. Blumberg Selinger and William M. Gelbart

*Department of Chemistry, University of California at Los Angeles, 405 Hilgard Avenue,  
Los Angeles, California 90024*

(Received 24 October 1990; revised manuscript received 1 February 1991)

Results are presented from molecular-dynamics simulations of ideal solids under conditions of constant temperature, pressure, and uniaxial tensile force. We show that the system remains in metastable equilibrium all the way up to a critical value of the applied stress or force, at which point it fails irreversibly via the nucleation of small-scale defects. The critical load (failure strength) is found to decrease strongly with temperature.

In the past decade several attempts have been made to study the stress-induced phase transitions and failure of ideal (i.e., defect-free) solids via finite-temperature molecular-dynamics simulation. Most notable is the pioneering work of Parrinello and Rahman<sup>1</sup> and Ray and Rahman<sup>2</sup> in which the constant pressure ensemble of Andersen<sup>3</sup> was systematically extended to include an anisotropic applied stress. Their primary interest, however, was to investigate the nature of crystal-crystal phase transformations in "ideal" metals under increasing tension or compression. Conversely, Soules and Busbey<sup>4</sup> have focused directly on the fracture process itself, examining, in particular, the plastic deformation via cavity formation in "pristine" glasses. But their studies were restricted to the case of fixed *strain* rather than imposed *stress*, and the systems simulated were finite in at least one dimension (i.e., microscopic "slabs" or "fibers"). Similarly, Kieffer and Angell<sup>5</sup> have considered isotropic expansions of silica networks in an effort to explore the fracture structures and dynamics induced by increasing negative pressure. Most recently, LaViolette has reported both amorphization and rupture<sup>6</sup> in Lennard-Jones solids, but again in the fixed volume (uniform strain) ensemble.

In the present work we exploit molecular-dynamics (MD) techniques to treat the failure of ideal solids subjected to uniaxial stress  $\sigma$  or tensile force  $f$  under conditions of fixed temperature and pressure. Most of our discussion and results will refer to the case of applied *force*, since our use of simulation methods for this ensemble appears to be novel. For sufficiently slow increase in applied load, the system is shown to evolve through a succession of metastable equilibria, up to a critical value  $f_E^c$  of the external ( $E$ ) force. For *subcritical* loads  $f_E$  close enough to  $f_E^c$  (i.e., within a few percent), the metastable state is observed to fail only after a time delay, whereas for  $f_E \gtrsim f_E^c$  this nucleation process is essentially instan-

aneous. For still smaller loads, the stressed solid remains metastable for *all* times of interest. While the system at  $f_E < f_E^c$  can be unloaded without hysteresis, it is seen to fail irreversibly (i.e., no recovery is possible via removal of applied tension) once the nucleation of microscopic defects has begun. Finally, the critical load—failure strength—is found to decrease significantly with temperature. This latter result, especially in the context of explicit microscopic simulation of the failure of single crystals, provides many additional insights into the role of thermal fluctuations in metastable solids. All of these findings are consistent with the statistical thermodynamic approach formulated via mean-field theory and model Monte Carlo calculations in a recent paper.<sup>7</sup>

We have employed two ensembles for our simulations, one involving fixed temperature ( $T$ ), pressure ( $P$ ), and stress ( $\sigma$ ), and the other fixed  $T, P$  and force ( $f$ ). These ensembles are generalizations and/or modifications of those proposed by Parrinello and Rahman<sup>1</sup> and Ray and Rahman,<sup>2</sup> inspired by the idea of (periodic-boundary condition) cell motion originally suggested by Andersen.<sup>3</sup> This fluctuating box is characterized instantaneously by its edge vectors, which—as columns—define a "shape matrix"  $\underline{h}$ . Each of the particle positions  $\mathbf{r}_i$  is normalized by this matrix according to  $\mathbf{r}_i = \underline{h} \mathbf{s}_i$ . The dynamical variables of the system are then comprised of the columns of  $\underline{h}$  and the scaled vectors  $\{\mathbf{s}_i\}$ . Let  $\underline{G}$  denote the metric tensor  $\underline{h}^T \underline{h}$ , with superscript  $T$  indicating a transpose in the usual way:  $r_{ij}^2 = \mathbf{r}_{ij}^T \mathbf{r}_{ij} = (\mathbf{s}_i - \mathbf{s}_j)^T \underline{G} (\mathbf{s}_i - \mathbf{s}_j)$ , for example, is the square of the distance between the  $i$ th and  $j$ th particles. Now, the system Lagrangian

$$\mathcal{L} = \frac{1}{2} \sum_{i=1}^N m_i \dot{\mathbf{s}}_i^T \underline{G} \dot{\mathbf{s}}_i - \sum_{1 \leq i < j \leq N} U(r_{ij}) + \frac{1}{2} W \text{Tr}(\dot{\underline{h}}^T \dot{\underline{h}}) - P \det|\underline{h}| \quad (1)$$

generates the following equations of motion for  $\underline{h}$  and  $\mathbf{s}_i$ :

$$\ddot{\mathbf{s}}_i = - \sum_{\substack{j=1 \\ (j \neq i)}}^N \frac{1}{m_i} (\phi'/r_{ij})(\mathbf{s}_i - \mathbf{s}_j) - \underline{G}^{-1} \dot{\underline{G}} \dot{\mathbf{s}}_i, \quad i=1,2,\dots,N \quad (2a)$$

$$\dot{\underline{h}} = \frac{1}{\mathcal{W}} (\underline{\sigma}_I - P \underline{I})(\underline{h}^{-1})^T \det|\underline{h}|. \quad (2b)$$

Here  $\mathcal{W}$  is a quantity with dimensions of mass (see below), and  $\underline{\sigma}_I$  is the internal stress tensor defined by

$$\underline{\sigma}_I = \frac{1}{\det|\underline{h}|} \left[ \sum_{i=1}^N m_i \mathbf{v}_i \mathbf{v}_i - \sum_{1 \leq i < j \leq N} (\phi'/r_{ij}) \mathbf{r}_{ij} \mathbf{r}_{ij} \right]. \quad (3)$$

The dynamics implied by the Lagrangian (1) have been shown<sup>1,2</sup> to result in a constant *enthalpy* when only hydrostatic pressure is applied. In the case of *nonisotropic* stress, however, subtle complications arise in attempting to identify a thermodynamic potential with the constant stress ensemble. Nevertheless, a meaningful statistical mechanics can be obtained by treating the external stress via the principle of virtual work.<sup>8</sup> The equations of motion so generated are identical in form to that of Eqs. (2a) and (2b), but with  $P \underline{I}$  now replaced by the full anisotropic stress tensor  $\underline{\sigma}_E$  which specifies the external load. In the special case of unidirectional load, we propose a constant-force ensemble, where the (external) *force*, rather than the stress, is fixed. Here we simply add a term  $-fh_3$  to the Lagrangian in (1), where  $h_3$  is the length of the repeating box edge along the direction of applied tension. This last ensemble *does* lead to a well-defined thermodynamic potential, in this case, a generalized enthalpy.<sup>9</sup> The two ensembles produce consistent results in the failure thresholds, stress-strain relations, etc. Accordingly, we present data alternately from these *two* ensembles, without further comment on the differences in thermodynamic formulations and equations of motion, etc.

We report results here for a pair interaction of the Lennard-Jones form:  $U(r) = 4\epsilon[(r_0/r)^{12} - (r_0/r)^6]$ . In terms of  $\epsilon$ ,  $r_0$ , and  $m$  ( $\equiv m_i$ , all  $i$ ), it is natural to introduce a characteristic time scale  $\tau \equiv (mr_0^2/\epsilon)^{1/2} = 0.5 \times 10^{-12}$  s, corresponding to  $m = 1 \times 10^{-22}$  g ( $\approx 60$  amu),  $r_0 = 2.5 \times 10^{-8}$  cm, and  $\epsilon = 2.5 \times 10^{-13}$  erg. Forces and stresses are measured in units of  $\epsilon/r_0$  and  $\epsilon/r_0^2$ , respectively. For  $\mathcal{W}$  we choose  $10m$ , but its value is immaterial since we consider only (metastable) equilibrium properties of the system.<sup>1-3</sup> In integrating the equations of motion for  $\{\mathbf{s}_i\}$  and  $\underline{h}$ , the time step is taken to be  $\Delta t = 0.0075\tau$ , using the standard predictor-corrector algorithm.<sup>10</sup> The temperature is kept constant by simple rescaling of the particle velocities every 40 steps. Consistent with the low vapor pressure (compared to atmospheric) of solids at the temperatures of our study, and the long-time scale for evaporation (relative to failure), we are free to set  $P=0$ . Uniaxial force or stress is applied at a constant rate  $\Delta f/\Delta t = 0.6$  or  $\Delta\sigma/\Delta t = 0.018$ , after first equilibrating the system (for  $5000\Delta t$ ) under zero load, starting from a two-dimensional, triangular, lattice with a nearest-neighbor distance of  $2^{1/6}r_0$ .

Figure 1(a) shows plots of the  $y$  (vertical) and  $x$  (hor-

izontal) components of the internal restoring force  $f_I$  for a system of 900 particles at  $kT=0.05\epsilon$  (henceforth written as  $T=0.05$ ) with external force applied along the  $y$  direction at a rate of 0.6. Note that  $f_I^x$  fluctuates about zero (since the system relaxes laterally to relieve stress), whereas  $f_I^y$  follows  $f_E$  with a slope of unity, indicating that the load is being increased slowly enough for the system to move through a succession of (metastable) equilibrium states. When the external force reaches a value of  $f_E = 108 \pm 1$ , however,  $f_I^y$  drops abruptly to zero. The corresponding value of the system's horizontal (lateral) length  $L_x$  is 33.1, implying a critical stress of  $\sigma_E^c = f_E^c/L_x^c = 3.3$ .

Failure of the system at  $\sigma_E \approx 3.3$  is indicated by an alternative criterion in Fig. 1(b), where we plot the vertical ( $yy$ ) and horizontal ( $xx$ ) components of the induced strain  $\epsilon$  for the same temperature, but with applied stress

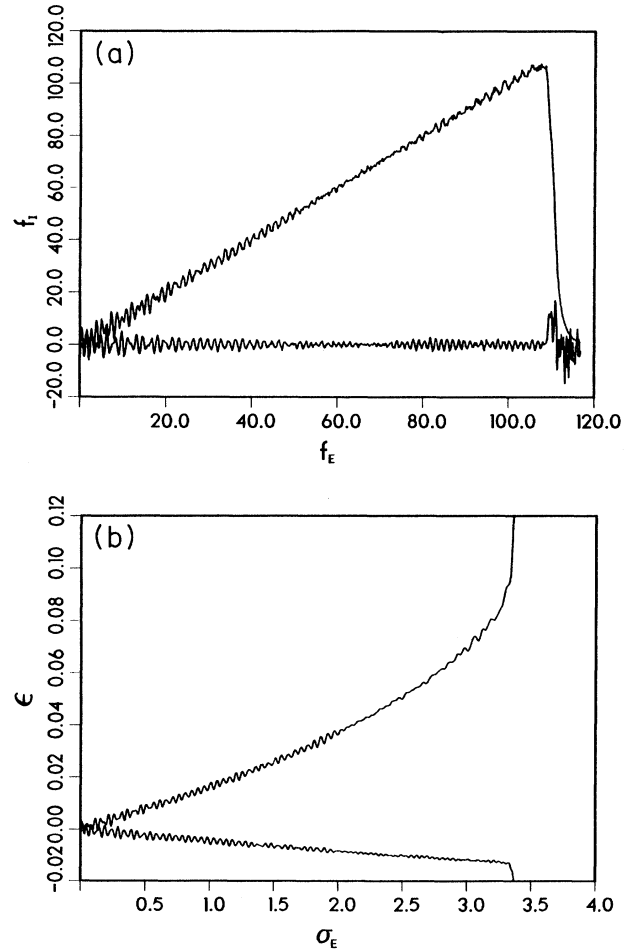


FIG. 1. (a) From the force-ensemble simulation at  $T=0.05$ , vertical (upper curve) and horizontal (lower curve) components of the internal force  $f_I$  vs the applied tensile force  $f_E$ . (b) Vertical (upper curve) and horizontal (lower curve) components of the strain tensor  $\epsilon$  vs the applied uniaxial stress  $\sigma_E$ , for the same temperature, but from the *stress* ensemble.

increasing at a rate of 0.018. For small stresses,  $\epsilon^{yy}$  increases linearly, with slope corresponding to the inverse of the elastic (Young's) modulus; nonlinearity sets in at larger  $\sigma_E$ , the anharmonicity of the pair potential beginning to be explored at this point. Finally,  $\epsilon^{yy}$  diverges at  $\sigma_E = 3.30 \pm 0.05$ , as the system fails. Note that the horizontal component  $\epsilon^{xx}$  is negative, indicating a positive Poisson ratio.

At higher temperature,  $T=0.2$ , we find a plot of  $f_I^y$  versus  $f_E$  which is essentially identical to Fig. 1(a), except that the system now fails earlier, at  $f_E = 63 \pm 1$ . The corresponding  $L_x$  is found to be 33.7, giving  $\sigma_E^c = 63/33.7 = 1.86$ . Similarly,  $\epsilon^{yy}$  versus  $\sigma_E$  at  $T=0.2$  has the same form as Fig. 1(b), except for the failure occurring at an external stress of 1.85; also, the inverse of the limiting slope (Young's modulus) is smaller than at the lower temperature. Thus, our estimates of the critical loads are confirmed by independent molecular-dynamics simulations carried out in the *force* and *stress* ensembles. Furthermore, these same failure stresses are found when we carried out similar calculations for a smaller system of 400 particles, as well as for slower increases in external load.

The foregoing results suggest that for sufficiently slow application of external stress or force, an ideal solid stays in quasi (metastable) equilibrium up to a critical load. This unique threshold corresponds to the failure of the system in the sense that the internal stress vanishes abruptly and the induced strain (in the direction of loading) diverges. And because the solid under stress is in a metastable state, thermal fluctuations play an important role in driving the intact system over its free energy barrier to failure. In particular, they are responsible for nucleating local inhomogeneities—point defects—at a characteristic rate which increases with both temperature and applied load.

More explicitly, consider a trajectory in the force ensemble simulations where we stop the increase of  $f_E$  and hold it fixed at a value near but below the failure threshold. The system is then subjected to this *particular* external force for 5000 time steps, i.e., for a time  $5000 \times 0.0075 = 37.5$ . Figure 2 shows how the *internal, restoring* force varies as time evolves over this interval for

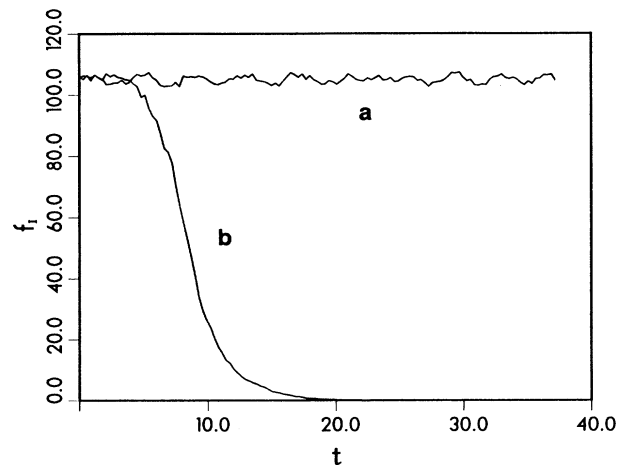


FIG. 2. From the force-ensemble simulation at  $T=0.05$ , the internal restoring force  $f_I$  vs time at two constant values of the applied force (a)  $f_E = 104.9$  and (b)  $f_E = 106.2$ .

each of two different values of the applied force at  $T=0.05$ . For  $f_E = 104.9$ , no change in  $f_I$  is observed: the internal force simply fluctuates about this applied value. For  $f_E = 106.2$ , however, the system remains in metastable equilibrium ( $f_I \approx f_E$ ) for a time  $t \approx 5$  and then fails abruptly.

Figure 3 shows a set of instantaneous particle configurations at different times corresponding to the  $f_E = 106.2$  trajectory in Fig. 2. Note that the starting configuration ( $t=0$ ) is remarkably regular, in spite of the fact that the applied tensile force is only 2% lower than the critical value ( $f_E^c \approx 108$ ) at which failure occurs instantaneously. After five time units, however, there is a clear development of defects—see, for example, a small opening near the lower right corner of Fig. 3(b) and several dislocation lines in the upper part. Figure 3(c) shows the particle configuration at  $t=7$ , by which time these “fatal” defects have begun to proliferate at an accelerated pace: it should be regarded as characterizing the *post-failure* regime, i.e., as lying beyond the limits of validity of the equilibrium molecular-dynamics method. Similar sequences of configurations are observed for *stress*

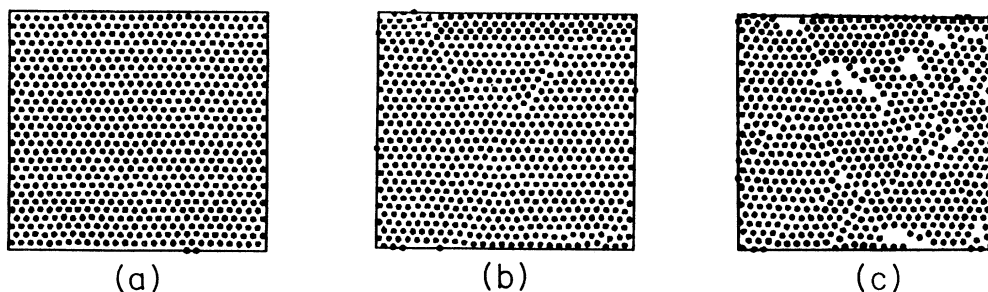


FIG. 3. From the force-ensemble simulation at  $T=0.05$ , instantaneous configurations showing nucleation and development of defects at applied uniaxial (vertical) force  $f_E = 106.2$ , at time (a)  $t=0$ , (b)  $t=5$ , (c)  $t=7$ .

ensemble runs just below the failure threshold, and at higher temperature. Decay of the metastable system via nucleation occurs after a time delay only if the applied load is close enough to its critical value (typically a few percent): above this narrow interval the system fails essentially instantaneously, while below it the metastable state survives effectively indefinitely, in close analogy<sup>7</sup> to the homogeneous condensation of a supersaturated vapor.

Consistent with the above scenarios, we expect the loading of our system to be reversible all the way up to its failure. To test this, we took the  $T=0.2$  system (for which  $f_E^c \approx 63$ ) up to an applied force of 60.3 and then abruptly released all of the load: after some transient oscillatory behavior, the system settles down to a state which is indistinguishable from the equilibrium configuration characteristic of  $f_E=0$ . On the other hand, the same system—kept at  $f_E=60.3$ —is found to fail after 1200 time steps. Furthermore, as soon as it begins to fail, i.e., even when the particle positions still reflect a conspicuously regular crystalline order apart from nascent openings and dislocations as noted in Fig. 3(b), *recovery is no longer possible* (regardless of how quickly—or slowly—the applied force is released). Thus we conclude that failure is irreversible as soon as microscopic defects first appear, even though the loading of the system is perfectly reversible all the way up to this point (e.g., no hysteresis in the stress-strain response, etc.).

To complement the *constant temperature* results discussed above, we also carried out computations under *adiabatic* conditions, to probe the failure behavior in the limit where the heat transfer rate is *slow* (rather than fast) compared to that of load increase. Starting from  $T=0.05$  and from 0.2, we find that the system temperature drops significantly as the external force is applied and, consequently, the failure threshold are pushed up to

higher values ( $117 \pm 1$  and  $73 \pm 1$ , versus  $108 \pm 1$  and  $63 \pm 1$ , respectively). We expect, however, that the temperatures at which the system fails in these cases are the same as those which would yield  $f_E^c=117$  and 73 in *isothermal* simulations. This check should provide another confirmation of the quasi(metastable) equilibrium nature of the prefailure regime. As far as we are aware, the dramatic temperature dependence reported here for the nucleation rates pertaining to failure of single crystals under tension is a feature of our MD approach. We also plan to study the effect of preexisting (i.e., zero-load) defects such as vacancies, substitutional impurities, and small-scale dislocation pairs, etc. (see, for example, Ref. 11 for the failure effects of quenched disorder) on plasticity and strength of these model solid systems, and to extend our simulations above the melting temperature in a probe of cavitation phenomena.<sup>5,12</sup>

We wish to thank Dr. C. L. Cleveland and Dr. M. W. Ribarsky for their assistance in carrying out the computations, and we especially thank Dr. Cleveland for providing us with the basic MD computer program. We also thank Professor H. Reiss for enlightening discussions. This research has been supported by a grant (No. DAAL03-89-K-0144) from the U.S. Defense Advanced Research Projects Agency, administered by the Army Research Office, and also by a grant (No. CHE88-16059) from the National Science Foundation; U.L. acknowledges support by a grant (No. FG-05-86ER45234) from the U.S. Department of Energy and a grant from the U.S. Air Force Office of Scientific Research; R.L.B.S. thanks the Office of the President of the University of California for support.

<sup>1</sup>M. Parrinello, Phys. Rev. Lett. **45**, 1196 (1980); J. Appl. Phys. **52**, 7182 (1980).

<sup>2</sup>J. R. Ray and A. Rahman, J. Chem. Phys. **80**, 4423 (1984).

<sup>3</sup>H. C. Andersen, J. Chem. Phys. **72**, 2384 (1980).

<sup>4</sup>T. F. Soules and R. F. Busbey, J. Chem. Phys. **78**, 6307 (1983).

<sup>5</sup>J. Kieffer and C. A. Angell, J. Non-Cryst. Solids **106**, 336 (1988).

<sup>6</sup>R. A. LaViolette, Phys. Rev. B **40**, 9952 (1989); (private communication).

<sup>7</sup>R. L. Blumberg Selinger, Z.-G. Wang, W. M. Gelbart, and A. Ben-Shaul, Phys. Rev. A **43**, 4396 (1991).

<sup>8</sup>M. W. Ribarsky and U. Landman, Phys. Rev. B **38**, 9522 (1988); C. L. Cleveland, J. Chem. Phys. **89**, 4987 (1988).

<sup>9</sup>H. Reiss, *Methods of Thermodynamics* (Blaisdell, New York, 1965).

<sup>10</sup>M. P. Allen and D. J. Tildesley, *Computer Simulation of Liquids* (Clarendon, Oxford, 1989).

<sup>11</sup>G. N. Hassold and D. J. Srolovitz, Phys. Rev. B **39**, 9273 (1989); W. A. Curtin and H. Scher, J. Mater. Res. **5**, 535 (1990); **5**, 554 (1990); A. Gilibert, C. Vanneste, D. Sornette, and E. Guyon, J. Phys. (Paris) **48**, 763 (1987).

<sup>12</sup>D. W. Oxtoby and R. Evans, J. Chem. Phys. **89**, 7521 (1988).